Research Article
J. Ginseng Res. Vol. 35, No. 1, 111-123 (2011)
DOI:10.5142/jgr.2011.35.1.111

JGR Journal of Ginseng Research

Microarray Analysis of Gene Expression by Ginseng Water Extracts in a Mouse Adrenal Cortex after Immobilization Stress

Young-Ock Kim* and Sang Won Lee

Medicinal Crops Division, Ginseng and Medicinal Plants Research Institute Rural Development Administration, Eumseong 369-873, Korea

To investigate the effects of repeated immobilization-stress challenge on the the hypothalamic–pituitary–adrenal axis, the genomic transcriptome in the adrenal cortex of immobilization-stressed mouse was analyzed by using a cDNA microarray. Mice were subjected to immobilization stress for 2 h per day for 5 consecutive d. With a 4.0-fold cutoff of arbitrary criteria, the expression levels of 168 out of 41,174 genes were significantly modulated in the adrenal cortex by stress when comparing the control and experimental groups. These genes were related to apoptosis, cell cycle, immune response, inflammatory responses, and signal transduction, and thus may be used as potential targets for the development of therapeutics for chronic stress or depression. Six significant genes among these were selected for real time polymerase chain reaction analysis to confirm the change of their expression levels. The gene for phospho 1 was also further investigated because its expression showed the greatest fold-change.

Keywords: *Panax ginseng*, Immobilization, Stress, Hypothalamic–pituitary–adrenal, Oligonucleotide array sequence analysis, Adrenal cortex

INTRODUCTION

Stress affects our daily lives. Many studies have shown that stress has profound effects on immunological parameters in humans and animals [1]. According to Cannon, homeostasis is the product of multiple physiological systems that maintain a steady-state in an organism [2]. Immobilization (IMO), a restraint stressor, is known to induce both psychological and physical stress which results in a wide range of behavioral and physiological alterations, secretion of stress hormones, and neuronal cell death in the brain [3]. Several research groups have reported on IMO stress-related changes in specific genes or proteins in organs such as stomach, liver, spleen, hippocampus, and the hypothalamic–pituitary–adrenal axis [4,5]. Corticotrophin releasing hormone is secreted by the hypothalamus and leads to the release of adrenocorticotropic hormone (ACTH) from the pituitary gland. ACTH causes the adrenal gland to synthesize and release catecholamines such as corticosterone, epinephrine, dopamine, and norepinephrine, which are all characteristic stress hormones.

Ginseng has a long history as a traditional medicine in Korea, China, and Japan. Recent studies have shown that ginseng increases resistance to stress, decreases blood pressure, benefits immune functions, and exerts antidepressant effects [6,7]. To date, approximately 70 kinds of saponin have been isolated from *Panax ginseng*. Most of these are protopanaxdiol and protopanaxtriol, which are aglycones of dammarane-type triterpenoids.

Recently, Cho *et al*. [8] acquired physicochemical

Received 20 Oct. 2010, **Revised** 12 Jan. 2011, **Accepted** 12 Jan. 2011

***Corresponding author**
E-mail: kyo9128@korea.kr
Tel: +82-43-871-5585, Fax: +82-43-871-5569

and spectroscopic data from four major diol-saponins: ginsenosides Rb1, Rb2, Rc, and Rd. Researche on the anti-stress effects of ginseng suggest that total ginseng saponins are the active components involved in the alleviation of mental and physical stress, and the normalization of work capacity [9]. However, the effects of ginseng on the adrenal cortex have not been studied.

DNA microarray technology, which has recently emerged as a powerful tool, allowed us to simultaneously analyze and compare gene expression in normal and treated cells [10]. We compared gene expression patterns in the adrenal cortex of mice either exposed or not exposed to restraint stress by ginseng treatment. Using oligo microarrays containing 44,000 genes of various functional classes, we found that 119 genes were up-regulated whereas 49 genes were down-regulated. We selected six genes of particular interest and confirmed the changes in the expression patterns of these genes by quantitative real time polymerase chain reaction (RT-PCR).

MATERIALS AND METHODS

Male CD-1(ICR) mice which were 6 wk old (Jung Ang, Seoul, Korea) were used for all experiments. The animals were randomly divided into four experimental groups and housed for at least 8 d prior to starting the experiments. They were kept on a 12-h light/dark cycle at a temperature of 23±1°C and given food and water *ad libitum*. The body weights of the mice were determined daily, immediately after exposure to 2 h of repeated IMO, using a digital balance (CAS, Seoul, Korea). The experimental procedures were carried out in accordance with the NIH Guide for Care and Use of Laboratory Animals, and were approved by the Kyung Hee University Institutional Animal Care and Use Committee.

For RT-PCR analysis, 1 μg of total RNA was reverse transcribed with 200 U of moloney murine leukemia virus (MMLV) reverse transcriptase (Life Technologies, Carlsbad, CA, USA), in 20 μL of reaction mixture containing random hexamers (Bioneer, Daejeon, Korea). One microliter of cDNA mixture was then used as DNA templates in 20 μL of reaction mixture containing 10 mM Tris–HCl (pH8.3), 50 mM KCl, 1.5 mM $MgCl_2$, 0.2 mM dNTP, 0.4 uM each primer, and 0.5 U *Taq* polymerase (TaKaRa, Shiga, Japan). RT-PCR was performed using a PTC-100 programmable thermal controller (MJ Research, Waltham, MA, USA). All primers were designed using web-based primer selection software, Primer 3 (The Whitehead Institute for Biomedical Research, Cambridge, MA, USA). The primer sequences and reaction conditions of the genes are shown in Table 5. The PCR products were separated on 1% agarose gels, stained with ethidium bromide, and photographed. The intensities of the bands were measured by ImageMaster VDS (Amersham Pharmacia, Buckinghamshire, UK) with ImageMaster TotalLab image-analyzing software. The signals of target PCR bands were normalized against the band intensity of glyceraldehyde-3-phosphate dehydrogenase. Data was expressed as the mean±standard error. Differences were analyzed with Student's *t*-test. A p-value of <0.05 was considered to be significant.

The ten mice of the IMO group were stressed daily by immobilization for 2 h in Rodent Restraint Cones (Stoelting, Wood Dale, IL, USA) which prevented all forward/backward and lateral movements. For repeated IMO stress, mice were immobilized at the same time every morning for five consecutive days. Mice were sacrificed by decapitation immediately after the 5th IMO stress treatment on the final day. The adrenal cortex was quickly removed and stored in cold RNAlater solution (Ambion, Austin, TX, USA) for further experimentation.

Real time polymerase chain reaction

Reverse transcription was performed using a TaqMan Reverse Transcription Regents Kit (Applied Biosystems, Foster City, CA, USA). The cDNA samples were diluted 1, 0.5, 0.25 0.125, and 0.0625 ng/mL. Triplet quantitative assays were performed on 1 mL of each cDNA dilution using the SYBR Green Master mix with an ABI 7900 sequence detection system according to the manufacture's protocol (Applied Biosystems). Gene-specific primers were designed by using PRIMEREX PRESS 1.0 software (Applied Biosystems) and are listed in Table 5.

Microarray analysis

For control and test RNAs, the synthesis of target cRNA probes and hybridization were performed using a Low RNA Input Linear Amplification kit (Agilent Technology, Santa Clara, CA, USA) according to the manufacturer's instructions. Briefly, 1 mg each of total RNA and T7 promoter primer was mixed and incubated at 65°C for 10 min. A cDNA master mix (5x first strand buffer, 0.1M DTT, 10 mM dNTP mix, RNase-Out, and MMLV-RT) was prepared and added to the reaction mixture. The samples were incubated at 40°C for 2 h, and then the RT and dsDNA synthesis was terminated by incubating the samples at 65°C for 15 min. The transcription master mix was prepared according to the manufacturer's protocol (4x transcription buffer, 0.1M DTT, NTP mix, 50% PEG, RNase-Out, inorganic pyrophosphatase, T7-

RNA polymerase, and cyanine 3/5-CTP). Transcription of dsDNA was performed by adding the transcription master mix to the dsDNA reaction samples and incubating at 40°C for 2 h Amplified and labeled cRNA was purified on cRNA Cleanup Module (Agilent Technology) according to the manufacturer's protocol. Labeled target cRNA was quantified using an ND-1000 spectrophotometer (NanoDrop Technologies Inc., Wilmington, DE, USA). After checking the labeling efficiency, fragmentation of cRNA was performed by adding 10x blocking agent and 25x fragmentation buffer, and incubating at 60°C for 30 min. The fragmented cRNA was resuspended in 2x hybridization buffer and directly pipetted onto an assembled Whole Rat Genome Oligo Microarray (44K; Agilent Technology). The arrays hybridized at 65°C for 17 h using an Agilent Hybridization oven (Agilent Technology). The hybridized microarrays were washed according to the manufacturer's washing protocol.

Data acquisition and analysis

The hybridized images were scanned using a DNA microarray scanner and quantified with Feature Extraction Software (Agilent Technology). All data normalization and selection of fold-changed genes were performed using GeneSpringGX 7.3 (Agilent Technology). Intensity-dependent normalization (locally-weighted regression scatterplot smoother) was performed where the ratio was reduced to the residual of the Lowess fit of the intensity versus the ratio curve. The averages of the normalized ratios were calculated by dividing the average of normalized signal channel intensity by the average of normalized control channel intensity. Functional annotation of the genes was performed using GeneSpringGX 7.3 according to the Gene Ontology Consortium. Gene classification was based on searches of BioCarta, GenMAPP, DAVID, and Medline databases.

RESULTS AND DISCUSSION

Microarray

Microarray analysis is a technique that has been shown to be useful for the simultaneous profiling of global gene expression and converging new genes or new functions of known genes [11]. For these reason, microarray analysis has been used to study gene expression in stressed mice following treatment with herbal medicine [12] and stress-related changes in gene expression following treatment with ginseng.

RNA quality

Preparation of highly pure undegraded total RNA is essential for performing a successful microarray. The quality of the total RNA was monitored with a RNA 6000 Pico Assay Solution using 2100 Bioanalyzer (Agilent Technology). No degradation was evident in the gel-like images of the control and sample preparations (Fig. 1A). The rRNA ratios (28S/18S) of each preparation were close to 2.0 (Fig. 1B). These data indicate that high-quality RNA was recovered.

MA-plot

An MA-plot of the microarray data, where M and A represent log2(Cy5 intensity/Cy3 intensity) and 1/2log2(Cy5 intensity×Cy3 intensity), respectively, is a plot of log-ratio of two expression intensities versus the mean log-expression of the two [13]. As shown in Fig. 2, most M values are between ±1.0, meaning that up- or down-regulation scales are mostly less than 2-fold.

Data processing

Array images were analyzed to check general signal intensities from the DNA chips after hybridization of the samples and probes on the chips (data not shown). After acquisition from the images, the signals were transformed into digital numbers and an analysis was performed. To test the reproducibility of each microarray analysis, the absolute data from each chip (data not shown) were compared. Normalization and comparison of the data were done and hierarchical clustering was performed.

Functional distribution and regulation of genes

Genes were classified into nine functional groups (immune response, neurogenesis, cell cycle, apoptosis, DNA repair, signal transduction, and gene transcription). The overall distribution of the genes in each groups that were up- or down-regulated by more than 2-fold following ginseng extract administration on the 5th day after IMO stress are shown in Fig. 3. There were more up-regulated (119) than down-regulated (49) genes. Lists of genes in each group are shown in Table 4.

Stress response–related genes (Table 1)

Defension beta 3 (Defβ3)

The Defβ3 gene was up-regulated by 4.2±0.16 fold. Mammalian cells express a number of peptide antibiotics as an innate host defense system [14]. Defensins and acathelicidin are the two major classes of antimicrobial peptides in humans [15]. Defensins are divided into α-and β-denfensins. In humans, α-denfensins are expressed in the small intestine (neurtophils and Paneth cells) whereas β-denfensins are mainly found in epithelial tissues.

A

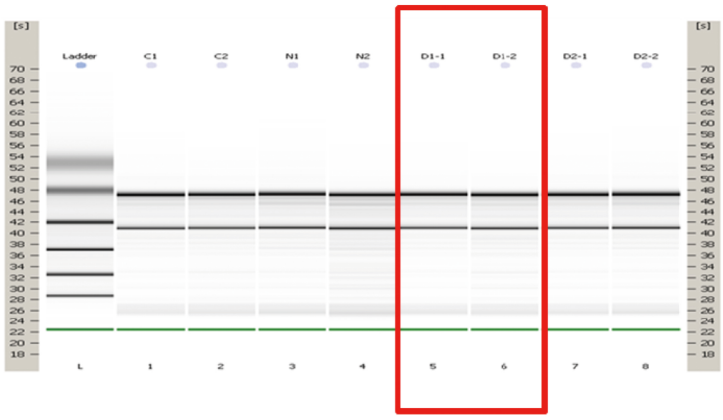

Lane	Sample name
1	C-1
2	C-2
3	N-1
4	N-2
5	Ginseng-1
6	Ginseng-2
7	D2-1
8	D2-2

B

Sample	μg/μL	$OD_{260/230}$	Total (μg)	Ratio(28s/18s)	RIN	Result
C-1	1.1536	2.2	56.5264	1.7	9.3	Pass
C-2	0.8589	2.1	40.3730	1.8	9.0	Pass
N-1	0.9118	2.0	42.8546	1.4	8.8	Check
N-2	1.7089	2.1	83.7361	1.2	8.0	Check
Ginseng-1	1.4637	2.2	68.7939	1.8	9.4	Pass
Ginseng-2	1.2945	2.0	59.5470	1.5	8.7	Check
D2-1	1.4560	2.3	66.9760	1.8	9.3	Pass
D2-2	1.1279	2.1	51.8834	1.5	9.0	Check

Fig. 1. RNA quality assessment. The quality of the RNA preparations was monitored using a RNA 6000 Pico Assay Solution and a 2100 Bioanalyzer (Agilent Technology). Gel-like images control and sample preparations (A) are shown. rRNA ratios (28S/18S ribosomal RNA) are shown in (B). (B) Data is from one of nine independent experiments. OD: optical density, RIN: RNA index number(1.0-10.0).

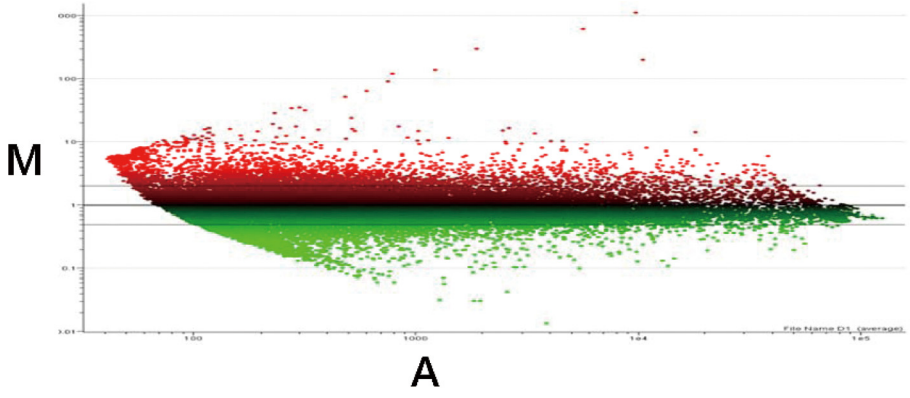

Fig. 2. The MA plot of the cDNA microarray hybridization. Gene expression signals of stressed mice and stressed mice treated with ginseng. Each point represents the average expression value for the same gene in stressed and non-stressed mice. MA plots were used to represent the R and G data, where M (relative expression ratio)=log2(CY5/CY3). A (signal intensity)=[log2(Cy5XCy3)]/2. G is the stronger control sample (stressed mice) hybridization (CY3) and R is the stronger experimental (stressed mice treated with ginseng) sample hybridization (CY5).

alpha-2-HS-glycoprotein (ahsg)

αhsg was down-regulated by 5.8±0.17 fold. αhsg is a serum glycoprotein. αhsg-KO mice show impaired tolerance to ischemia suggesting that ahsg exerts a protective effect against ischemia in cardiomyocytes [16].

Up-regulated immune response–related genes (Table 2)

Colony stimulating factor 3 (Csf3)

The Csf3 gene was up-regulated by 19.62-fold. G-CSF stimulates the expression of the MIP-2 receptor via STAT3-dependent transcriptional activation of Il8rb [17].

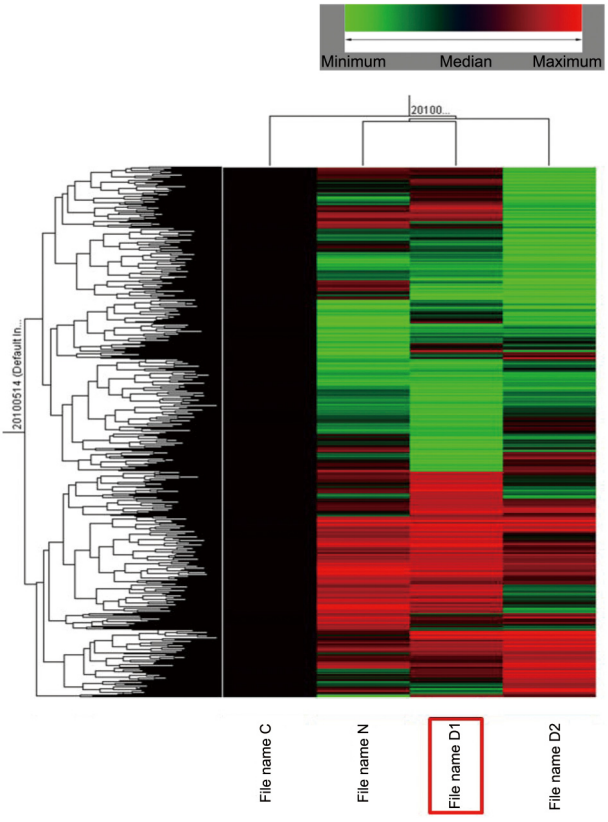

Fig. 3. Functional distribution of regulated genes. The overall distribution of the genes in each group which were up-regulated (A) or down-regulated (B) by a factor greater than 2-fold following ginseng extract administration on the 5th day after the immobilization challenge.

G-CSF and IL-6 provide signals that determine the angiogenic potential of resident monocytes in BM [18].

C-type lectin domain family 4, member a2 (Clec4a2)

The Clec4a2 gene was up-regulated by 5.90-fold. This observation indicates that Dcir is a negative regulator of dendritic cell expansion and has a crucial role in maintaining the homeostasis of the immune system [19].

Radical S-adenosyl methionine domain containing 2 (Rsad2)

The Rsad2 gene was up-regulated by 10.60-fold. Viperin may play a central role in bacterial or parasitic infections, and may protect neutrophils and macrophages from infection [20].

Up-regulated cell cycle response–related genes (Table 3)

Centromere autoantigen H (Cenph)

The Cenph gene was up-regulated by 14.34-fold. TRIM36 interacts with the kinetochore protein CENP-H and delays cell cycle progression [21]. Immunocytochemical analysis of CENP-I-deficient cells demonstrated that both CENP-I and CENP-H are necessary for localization of CENP-C, but not CENP-A, to the centromere [22].

Nusap1 protein (Nusap1)

The Nusap1 gene was up-regulated by 13.26-fold. NuSAP is essential for proliferation of embryonic cells and, simultaneously, they underscore the importance of chromatin-induced spindle assembly [23].

Integrin beta 1D (Itgβ1)

The Nusap1 gene was up-regulated by 13.26-fold. Ablation of beta1 integrin induces organ atrophy by disrupting acinar cell polarity and exposing the pancreatic parenchyma to digestive enzymes [24].

Up-regulated apoptosis response–related genes (Table 4)

N-acylsphingosine amidohydrolase 2 (Asah2)

Asah2 was up-regulated by 15.87-fold. Asah2 is an N-acylsphingosine amidohydrolase 2. Expression of this enzyme is decreased in the small intestine in transgenic mice lacking CFTR [25]. The Asah2-encoded neutral ceramidase is a key enzyme for the catabolism of dietary sphingolipids and regulates the levels of bioactive sphingolipid metabolites in the intestinal tract [26].

Fibroblast growth factor receptor 1 isoform 1 (Fgfr1)

Fgfr1 was up-regulated by 15.64-fold. This result indicates that MAPK/ERK activation downstream of FGFR1 is necessary for motor axon guidance, and that embryonic stem cell-derived neurons provide an important tool for dissecting intracellular pathways required for axon guidance [27]. FGFR1 is indispensable for complete differentiation and activation of osteoclasts in mice [28]. Dysfunctions in glial cells and FGF receptor signaling may therefore be implicated in neurodegenerative hearing loss associated with the normal aging process [29].

Eukaryotic translation elongation factor 1 alpha 2 (Edf1a2)

Edf1a2 was up-regulated by 15.24-fold. Eefla 2 interacts with Prdx-I to provide cells with extraordinary resistance to oxidative stress-induced cell death [30]. Expression of eEF1A-2/S1 protein is activated upon myogenic differentiation [31].

Despite these DNA microarray studies on stress response, no novel IMO stress-related genes were discovered. In this study, to search the novel genes which were up- or down-regulated by IMO stress in the mouse's adrenal cortex, the transcriptional activity of the adrenal cortex in mice challenged with days of repeated IMO

Table 1. Immobilization stress-related changes in gene expression in the adrenal cortex

GenBank ID	Fold	Gene	Function
NM_153082	15.0±0.02↑	C330021A05Rik	DnaJ (Hsp40) homolog, subfamily C, member 27
NM_183027	14.9±0.15↑	Ap1s3	Adaptor-related protein complex AP-1, sigma 3
BC021475	10.5±0.49↑	2610301G19Rik	RIKEN cDNA 2610301G19 gene
NM_153104	10.3±0.31↑	Phospho1	Phosphatase, orphan 1
NM_145929	10.1±0.12↑	Gga1	Golgi associated, gamma adaptin ear containing, ARF binding protein 1
NM_011548	10.0±0.04↑	Tcfe2a	Transcription factor E2a
NM_009700	9.3±0.28↑	Aqp4	Aquaporin 4
NM_029021	9.2±0.21↑	4833422F24Rik	RIKEN cDNA 4833422F24 gene
NM_001031814	9.0±0.04↑	2610207I05Rik	SMG1 homolog, phosphatidylinositol 3-kinase-related kinase (C. elegans)
NM_009545	7.5±0.50↑	Pcgf2	Polycomb group ring finger 2
NM_020587	7.4±0.45↑	Sfrs4	Splicing factor, arginine/serine-rich 4 (SRp75)
AK048180	7.2±0.17↑	Spata5l1	Spermatogenesis associated 5-like 1
NM_175204	7.0±0.00↑	5830406J20Rik	Proteasome (prosome, macropain) subunit, beta type, 11
AK005867	6.8±0.21↑	1700011H22Rik	RIKEN cDNA 1700011H22 gene
AK049020	6.8±0.23↑	9630031F12Rik	Family with sequence similarity 184, member B
NM_026174	6.6±0.37↑	Entpd4	Ectonucleoside triphosphate diphosphohydrolase 4
NM_177730	6.6±0.44↑	Impad1	Inositol monophosphatase domain containing 1
NM_011278	6.5±0.48↑	Rnf4	Ring finger protein 4
NM_172758	6.5±0.48↑	BC031853	Solute carrier family 38, member 7
NM_021295	6.5±0.48↑	Lancl1	LanC (bacterial lantibiotic synthetase component C)-like 1
NM_146492	6.4±0.40↑	Olfr724	Olfactory receptor 724
NM_020255	6.3±0.32↑	Scand1	SCAN domain-containing 1
NM_146683	6.3±0.28↑	Olfr1441	Olfactory receptor 1441
NM_175557	6.3±0.27↑	Zfp384	Zinc finger protein 384
NM_134226	6.3±0.26↑	V1rj2	Vomeronasal 1 receptor, J2
NM_001037712	6.2±0.20↑	Kcnh6	Potassium voltage-gated channel, subfamily H (eag-related), member 6
NM_009401	6.2±0.16↑	Tnfrsf8	Tumor necrosis factor receptor superfamily, member 8
NM_009392	6.1±0.14↑	Tlx2	T-cell leukemia, homeobox 2
NM_146892	6.1±0.13↑	Olfr1223	Olfactory receptor 1223
AK036614	6.1±0.08↑	02-Mar	Membrane-associated ring finger (C3HC4) 2
NM_145857	6.1±0.05↑	Nod2	Nucleotide-binding oligomerization domain containing 2
NM_001010941	6.0±0.01↑	Gpr12	G-protein coupled receptor 12
NM_013855	5.9±0.07↑	Abca3	ATP-binding cassette, sub-family A (ABC1), member 3
NM_030725	5.8±0.19↑	Syt13	Synaptotagmin XIII
NM_198621	5.8±0.21↑	Gm443	Predicted gene 443
NM_010438	5.6±0.38↑	Hk1	Hexokinase 1
NM_011348	5.6±0.38↑	Sema3e	Sema domain, immunoglobulin domain (Ig), short basic domain, secreted, (semaphorin) 3E
NM_021535	5.6±0.39↑	Smu1	Smu-1 suppressor of mec-8 and unc-52 homolog (C. elegans)
NM_007577	5.6±0.40↑	C5ar1	Complement component 5a receptor 1
NM_001011820	5.4±0.40↑	Olfr1359	Olfactory receptor 1359
NM_012028	5.4±0.39↑	St6galnac5	ST6 (alpha-N-acetyl-neuraminyl-2,3-beta-galactosyl-1,3)-N-acetylgalactosaminide alpha-2,6-sialyltransferase 5
NM_027427	5.3±0.35↑	Taf15	TAF15 RNA polymerase II, TATA box binding protein (TBP)-associated factor
NM_207685	5.3±0.34↑	Elavl2	ELAV (embryonic lethal, abnormal vision, Drosophila)-like 2 (Hu antigen B)
NM_175263	5.3±0.33↑	5730593N15Rik	Notum pectinacetylesterase homolog (Drosophila)

Table 1. Continued-1

GenBank ID	Fold	Gene	Function
NM_029607	5.3±0.28↑	2310003C23Rik	RIKEN cDNA 2310003C23 gene
NM_146206	5.3±0.26↑	Tpcn2	Two pore segment channel 2
NM_023117	5.2±0.20↑	Cdc25b	Cell division cycle 25 homolog B (S. pombe)
NM_053185	5.2±0.19↑	Col4a6	Collagen, type IV, alpha 6
NM_026976	5.2±0.17↑	Faim3	Fas apoptotic inhibitory molecule 3
AK042979	5.2±0.16↑	Tbc1d4	TBC1 domain family, member 4
NM_146709	5.2±0.16↑	Olfr411	Olfactory receptor 411
NM_019826	5.1±0.11↑	Ivd	Isovaleryl coenzyme A dehydrogenase
NM_029090	5.1±0.09↑	1200013P24Rik	N-acetyltransferase 15 (GCN5-related, putative)
NM_032397	5.0±0.04↑	Kcnn1	Potassium intermediate/small conductance calcium-activated channel, subfamily N, member 1
NM_172641	5.0±0.03↑	9930023K05Rik	RIKEN cDNA 9930023K05 gene
NM_183148	5.0±0.02↑	C79267	Intermediate filament family orphan 2
NM_027100	4.9±0.06↑	Rwdd2	RWD domain containing 2A
NM_178666	4.9±0.06↑	E430004N04Rik	Thymocyte selection pathway associated
NM_029001	4.9±0.06↑	Elovl7	ELOVL family member 7, elongation of long chain fatty acids (yeast)
NM_019553	4.9±0.13↑	Ddx21	DEAD (Asp-Glu-Ala-Asp) box polypeptide 21
NM_008267	4.8±0.16↑	Hoxb13	Homeo box B13
NM_026668	4.8±0.22↑	4930558O21Rik	Leucine-rich repeats and IQ motif containing 4
NM_147069	4.8±0.23↑	Olfr686	Olfactory receptor 686
NM_198614	4.7±0.28↑	4932409I22Rik	Family with sequence similarity 148, member C
NM_001039169	4.7±0.30↑	Eif4e2	Eukaryotic translation initiation factor 4E member 2
NM_026470	4.7±0.31↑	Spata6	Spermatogenesis associated 6
NM_146653	4.7±0.32↑	Olfr435	Olfactory receptor 435
BC048580	4.7±0.32↑	Brpf3	Bromodomain and PHD finger containing, 3
NM_177164	4.7±0.33↑	A830006F12Rik	RIKEN cDNA A830006F12 gene
AK084222	4.7±0.34↑	2700094F01Rik	Transmembrane protein 209
NM_178773	4.7±0.35↑	Tmem16d	Anoctamin 4
NM_029413	4.6±0.37↑	Morc4	Microrchidia 4
NM_031376	4.6±0.37↑	Pik3ap1	Phosphoinositide-3-kinase adaptor protein 1
XM_975192	4.6±0.39↑	Camsap1	Calmodulin regulated spectrin-associated protein 1
NM_183316	4.6±0.41↑	Snapc5	Small nuclear RNA activating complex, polypeptide 5
NM_022320	4.6±0.41↑	Gpr35	G protein-coupled receptor 35
AK045799	4.6±0.43↑	Fhad1	Forkhead-associated (FHA) phosphopeptide binding domain 1
XM_888058	4.6±0.44↑	C330016K18Rik	Solute carrier family 4, sodium bicarbonate cotransporter, member 5
NM_009233	4.5±0.47↑	Sox1	SRY-box containing gene 1
NM_001013823	4.5±0.49↑	LOC435285	Keratin associated protein 4-16
NM_175445	4.5±0.48↑	Rassf2	Ras association (RalGDS/AF-6) domain family member 2
NM_028065	4.5±0.48↑	Tnrc5	Canopy 3 homolog (zebrafish)
NM_080452	4.5±0.48↑	Mrps2	Mitochondrial ribosomal protein S2
NM_147109	4.5±0.47↑	Olfr577	Olfactory receptor 577
NM_010746	4.5±0.45↑	Ncr1	Natural cytotoxicity triggering receptor 1
NM_134249	4.5±0.45↑	Timd2	T-cell immunoglobulin and mucin domain containing 2
NM_008470	4.4±0.41↑	Krt16	Keratin 16
NM_001038590	4.4±0.38↑	Cldn19	Claudin 19

Table 1. Contined-2

GenBank ID	Fold	Gene	Function
NM_145388	4.4±0.38↑	Best2	Bestrophin 2
NM_025834	4.4±0.37↑	Proz	Protein Z, vitamin K-dependent plasma glycoprotein
XM_619828	4.4±0.36↑	Scrt2	Scratch homolog 2, zinc finger protein (Drosophila)
AK145379	4.4±0.36↑	H19	H19 fetal liver mRNA
NM_011487	4.3±0.35↑	Stat4	Signal transducer and activator of transcription 4
NM_001039365	4.3±0.32↑	Mobp	Myelin-associated oligodendrocytic basic protein
NM_008865	4.3±0.30↑	Csh2	Prolactin family 3, subfamily b, member 1
NM_019940	4.3±0.29↑	Zfp111	Zinc finger protein 111
NM_010085	4.3±0.27↑	Adam26a	A disintegrin and metallopeptidase domain 26A (testase 3)
AK002926	4.3±0.25↑	Klf13	Kruppel-like factor 13
AK044798	4.2±0.25↑	Atg4d	Autophagy-related 4D (yeast)
NM_029781	4.2±0.24↑	Rab36	RAB36, member RAS oncogene family
NM_153805	4.2±0.24↑	Pkn3	Protein kinase N3
NM_147110	4.2±0.23↑	Olfr570	Olfactory receptor 570
NM_020287	4.2±0.21↑	Insm2	Insulinoma-associated 2
NM_027069	4.2±0.21↑	1700018F24Rik	RIKEN cDNA 1700018F24 gene
AK008094	4.2±0.17↑	Igl-V1	Immunoglobulin lambda chain, variable 1
NM_182636	4.2±0.17↑	BC052055	von Willebrand factor A domain containing 5B2
NM_010828	4.2±0.17↑	Cited2	Cbp/p300-interacting transactivator, with Glu/Asp-rich carboxy-terminal domain, 2
NM_199313	4.2±0.17↑	AY053573	Retinol dehydrogenase 18
NM_139225	4.2±0.16↑	Defb10	Defensin beta 10
AK033743	4.1±0.10↑	Lcn6	Lipocalin 6
NM_172896	4.1±0.09↑	Nalp4a	NLR family, pyrin domain containing 4A
NM_010407	4.1±0.07↑	Hck	Hemopoietic cell kinase
NM_026893	4.1±0.07↑	Wdr40a	WD repeat domain 40A
NM_175225	4.1±0.05↑	Tasp1	Taspase, threonine aspartase 1
NM_009567	4.0±0.05↑	Zfp93	Zinc finger protein 93
NM_139296	4.0±0.04↑	Moxd2	Monooxygenase, DBH-like 2
NM_008498	4.0±0.01↑	Lhx1	LIM homeobox protein 1
NM_173405	4.0±0.01↑	6530401C20Rik	Archaelysin family metallopeptidase 1
NM_138630	4.0±0.00↑	Arhgap4	Rho GTPase activating protein 4
NM_008577	4.1±0.24↓	Slc3a2	Solute carrier family 3 (activators of dibasic and neutral amino acid transport), member 2
NM_007981	4.2±0.24↓	Acsl1	Acyl-CoA synthetase long-chain family member 1
NM_008645	4.2±0.24↓	Mug1	Murinoglobulin 1
NM_031188	4.2±0.24↓	Mup1	Major urinary protein 1
NM_008407	4.2±0.24↓	Itih3	Inter-alpha trypsin inhibitor, heavy chain 3
NM_019423	4.2±0.24↓	Elovl2	Elongation of very long chain fatty acids (FEN1/Elo2, SUR4/Elo3, yeast)-like 2
NM_009654	4.2±0.24↓	Alb1	Albumin
NM_080434	4.4±0.23↓	Apoa5	Apolipoprotein A-V
NM_013820	4.4±0.23↓	Hk2	Hexokinase 2
BC037152	4.4±0.23↓	Mup1	Major urinary protein 1
NM_054094	4.4±0.23↓	Acsm1	Acyl-CoA synthetase medium-chain family member 1
NM_009876	4.5±0.22↓	Cdkn1c	Cyclin-dependent kinase inhibitor 1C (P57)
NM_008646	4.5±0.22↓	Mug2	C3 and PZP-like, alpha-2-macroglobulin domain containing 8

Table 1. Contined-3

GenBank ID	Fold	Gene	Function
NM_010006	4.5±0.22↓	Cyp2d9	Cytochrome P450, family 2, subfamily d, polypeptide 9
NM_010559	5.0±0.20↓	Il6ra	Interleukin 6 receptor, alpha
NM_146148	5.0±0.20↓	C8a	Complement component 8, alpha polypeptide
NM_174870	5.0±0.20↓	Slc26a1	Solute carrier family 26 (sulfate transporter), member 1
NM_144511	5.1±0.20↓	EG13909	Esterase 31
NM_008986	5.1±0.19↓	Ptrf	Polymerase I and transcript release factor
NM_145356	5.2±0.19↓	Zbtb7c	Zinc finger and BTB domain containing 7C
NM_007817	5.2±0.19↓	Cyp2f2	Cytochrome P450, family 2, subfamily f, polypeptide 2
NM_011315	5.2±0.19↓	Saa3	Serum amyloid A 3
NM_008819	5.2±0.19↓	Pemt	Phosphatidylethanolamine N-methyltransferase
AK028683	5.4±0.18↓	Cps1	Carbamoyl-phosphate synthetase 1
NM_023114	5.4±0.18↓	Apoc3	Apolipoprotein C-III
NM_017399	5.5±0.18↓	Fabp1	Fatty acid binding protein 1, liver
NM_144903	5.7±0.18↓	Aldob	Aldolase B, fructose-bisphosphate
NM_010005	5.8±0.17↓	Cyp2d10	Cytochrome P450, family 2, subfamily d, polypeptide 10
NM_013465	5.8±0.17↓	Ahsg	Alpha-2-HS-glycoprotein
NM_010210	5.8±0.17↓	Fhit	Fragile histidine triad gene
NM_019792	6.1±0.16↓	Cyp3a25	Cytochrome P450, family 3, subfamily a, polypeptide 25
NM_010004	6.1±0.16↓	Cyp2c40	Cytochrome P450, family 2, subfamily c, polypeptide 40
NM_144903	6.2±0.16↓	Aldob	Aldolase B, fructose-bisphosphate
NM_029821	6.3±0.16↓	1190003J15Rik	RIKEN cDNA 1190003J15 gene
NM_011707	6.3±0.16↓	Vtn	Vitronectin
NM_023114	6.3±0.16↓	Apoc3	Apolipoprotein C-III
NM_198615	6.4±0.16↓	Rkhd1	Mex3 homolog D (C. elegans)
NM_011314	6.6±0.15↓	Saa2	Serum amyloid A 2
AK082385	7.3±0.14↓	Indol1	Indoleamine 2,3-dioxygenase 2
NM_017371	7.5±0.13↓	Hpxn	Hemopexin
NM_011458	7.8±0.13↓	Serpina3k	Serine (or cysteine) peptidase inhibitor, clade A, member 3K
NM_011316	8.1±0.12↓	Saa4	Serum amyloid A 4
NM_011458	9.1±0.11↓	Serpina3k	Serine (or cysteine) peptidase inhibitor, clade A, member 3K
NM_007870	9.2±0.11↓	Dnase1l3	Deoxyribonuclease 1-like 3
NM_017473	9.4±0.11↓	Rdh7	Retinol dehydrogenase 7
BC037008	9.6±0.10↓	Serpina1b	Serine (or cysteine) preptidase inhibitor, clade A, member 1B
NM_009245	9.7±0.10↓	Serpina1c	Serine (or cysteine) peptidase inhibitor, clade A, member 1C
NM_009512	9.8±0.10↓	Slc27a5	Solute carrier family 27 (fatty acid transporter), member 5
NM_010168	10.0±0.10↓	F2	Coagulation factor II

↑ and ↓ indicate the up- and down-regulation of gene expression. 4.0↓ means that the expression level was decreased to 1/4.

was quantitatively analyzed using cDNA microarray. After sacrificing the mice on the last day of the IMO stress challenge, the adrenal cortex was quickly separated from the adrenal gland and used for the purification of total RNA. The significantly up- or down-regulated genes were identified using the following criteria: significant difference between the control and IMO groups, that is, $p<0.05$ (*t*-test) and a mean fold-change >1.5. A fluctuation in gene expression levels over 4-fold was considered to be sufficient to induce significant biochemical

Table 2. Immune response-related genes

GenBank ID	Fold	Gene	Function
A_51_P317176	19.62196	Csf3	Colony stimulating factor 3 (granulocyte)
A_52_P356106	15.894692	Clec4a2	C-type lectin domain family 4, member a2 C-type lectin domain family 4, member a2
A_51_P505134	10.594688	Rsad2	Radical S-adenosyl methionine domain containing 2
A_52_P560113	10.428145	H2-Bl	Histocompatibility 2, blastocyst
A_52_P651316	8.93424	Cd79a	CD79A antigen (immunoglobulin-associated alpha)
A_51_P166941	8.156842	Irak3	Interleukin-1 receptor-associated kinase 3
A_52_P66520	7.9745355	Clec12a	C-type lectin domain family 12, member a
A_52_P100926	7.9733095	Il1a	Interleukin 1 alpha
A_51_P168115	7.8946457	Il21	Interleukin 21
A_51_P335945	7.8921895	Pag1	Phosphoprotein associated with glycosphingolipid microdomains 1
A_51_P512085	7.79134	Colec12	Collectin sub-family member 12
A_52_P641747	7.7182136	Sh2d1a	SH2 domain protein 1A
A_51_P464703	7.5314245	Ccl8	Chemokine (C-C motif) ligand 8
A_51_P328537	7.4499946	Eda	Ectodysplasin-A
A_52_P523946	7.4396567	Ddx58	DEAD (Asp-Glu-Ala-Asp) box polypeptide 58
A_51_P436652	7.33316	Ccl7	Chemokine (C-C motif) ligand 7

Table 3. Cell cycle-related genes

GenBank ID	Fold	Gene	Function
A_51_P404766	14.9005575	Tlk2	
A_51_P492830	14.337363	Cenph	Centromere autoantigen H
A_52_P69281	13.263976	Nusap1	Nusap1 protein
A_51_P302527	12.605151	Nek1	
A_52_P69236	11.924297	Itgb1	Integrin beta1D
A_51_P340003	11.358889	Sycp1	Synaptonemal complex protein 1
A_51_P419169	10.672192	Suv39h2	Suppressor of variegation 3-9 homologue 2
A_52_P615877	10.460364	Cdc25b	Cell division cycle 25 homolog B
A_52_P259250	9.951616	Evi5	Ecotropic viral integration site 5
A_52_P131891	9.72852	Spag5	Sperm associated antigen 5
A_52_P512955	9.418641	Anln	Anillin
A_51_P475523	9.060346	Brca1	Breast cancer 1
A_52_P417489	8.984837	Cdk6	Cyclin-dependent kinase 6
A_52_P513394	8.50183	Brca2	Breast cancer 2
A_52_P404570	8.478805	Dbf4	Dbf4 protein
A_51_P369056	8.123366	Prox1	Prospero-related homeobox 1

and physiological changes in living cells. By using these criteria, 176 genes out of 41,174 genes were selected since their expression levels were significantly modulated in adrenal cortex by stress. 118 genes were up-regulated by IMO stress while 49 genes were down-regulated. Genes related to immune responses, apoptosis, and signal transduction were activated by a factor of 1.5 to 15.0 (Table 2). The expression of specific disease-related genes, such as Aqp4 (spinal cord injury), was strongly stimulated by stress. Among the up-regulated genes, nine olfactory receptors including Olfr 724, Olfr 1441, Olfr 1223, Olfr 1359, Olfr 411, Olfr 686, Olfr 435, Olfr 577, and Olfr 570 were highly overexpressed. mRNA processing genes, such as splicing factor, arginine/serine-rich 4 (Sfrs4), was also up-regulated over 7.4-fold. A majority of the up-regulated genes were found to be involved in transcriptional regulation (Tcfe2a, Stat4), or were cell signaling molecules (Camsap1) and receptors (V1rj2, Tnfrsf8, Gpr12, C5ar1, Gpr35, and Ncr1).

Table 4. Apoptosis-related genes

GenBank ID	Fold	Gene	Function
A_52_P56792	15.868544	Asah2	N-acylsphingosine amidohydrolase 2
A_52_P552062	15.643426	Fgfr1	Fibroblast growth factor receptor 1 isoform 1
A_51_P485862	15.239337	Eef1a2	Eukaryotic translation elongation factor 1 alpha 2
A_52_P401473	14.617006	Ntn1	
A_52_P403582	13.489419	Trim39	Tripartite motif protein 39
A_52_P131353	9.06976	Camk1d	Calcium/calmodulin-dependent protein kinase 1D
A_51_P475523	9.060346	Brca1	Breast cancer 1
A_52_P513394	8.50183	Brca2	Breast cancer 2
A_52_P282110	8.444962	Mef2c	
A_51_P484880	8.224829	Bcl2l11	BCL2-like 11 apoptosis facilitator isoform 1
A_51_P166941	8.156842	Irak3	Interleukin-1 receptor-associated kinase 3
A_52_P204710	8.133725	Sgk3	
A_51_P173285	7.8557196	Nkx2-5	NK2 transcription factor related, locus 5
A_51_P216550	7.837571	Trp63	Transformation related protein 63
A_51_P248935	7.737255	Terc	
A_52_P330424	7.6651587	Il2ra	

It was reported that restraint stress often modulates the immune system by either immunoactivation or immunosuppression depending on the intrinsic properties of the stress. Acute stress basically enhances the immune system to protect the body from stress-related dysfunction, whereas chronic stress gradually reduces overall immunity by inducing apoptotic death of immune cells and suppressing the basal expression of survival genes such as tumor suppressors, chaperones, and neurotrophin. In order to verify the gene expression levels obtained from the microarray analysis, six genes were selected for mRNA expression profiling by RT-PCR. Values from RT-PCR analyses are expressed as the mean and standard deviation from at least three independent experiments. The expression levels of five of these genes were found to decrease, but in case of phospho 1 the expression increased, which concurred with the microarray experiment results (Fig. 4).

The effects of IMO stress on the six genes demonstrated by RT-PCR are shown in Table 5. There were significant decreases in the cortical mRNA expression of

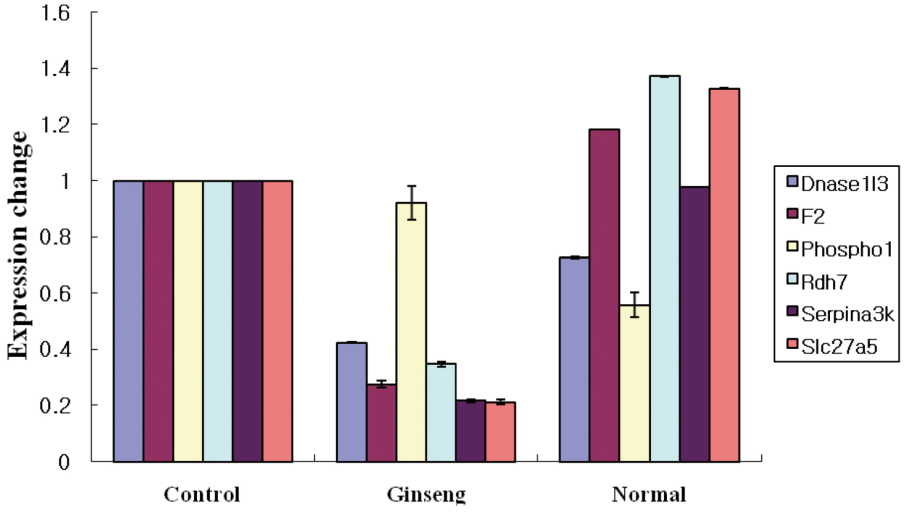

Fig. 4. Real-time polymerase chain reaction (PCR) analyses of immobilization stress-related genes in the adrenal cortex. The expression level of each target PCR product was normalized to that of glyceraldehyde-3-phosphate dehydrogenase, a house-keeping gene. Values are means and standard deviations from at least three independent experiments.

Table 5. Sequences of the primers used for real-time polymerase chain reaction

Gene name	Forward primer sequence	Reverse primer sequence	Size (bp)
Serpina3k	AAG GAA GTC TTC ACC GAA CAA G	GCC TTA CGA ATG CCA CCA ATA AC	155
Dnase1l3	GAG TGT TTG CTC CCT TCC TG	GGT TGC TTC TGA GAC TGG GA	193
F2	CAA CAT GTT CTG TGC TGG CT	TAC CAG CGG TTG TTA AAG GG	111
Slc27a5	GCC TAT GCC ACA CCT CAT TT	GGT TCC TTC ACA CAC AGC CT	198
Phospho1	GCT GTC TAC GAG ACC ATC CC	GAG CCC TGT TTG GCT ATG AA	71
Rdh7	CAC CTA GGA TGA GCT TTG CC	AAC GGC ATT AGG ATG TGG AG	150

five out of the six genes (Serpina 3K, Dnase113, F2, Slc27a5, and Rdh7) after the mice were subjected to IMO stress for 1 h. However, the cortical mRNA expression of phospho 1 was significantly increased in. The phospho1 gene is highly expressed in bone tissue, and phospho 1 protein localization is restricted to sites of skeletal mineralization in the mouse. Furthermore, phospho1 protein is cytosolic and active within murine osteoblasts [32,33]. Thrombin plays a major role in extra-intestinal thrombus formation associated with experimentally-induced colitis. It also appears to contribute to the propagation/stabilization, rather than initiation, phase of colitis-associated thrombogenesis at distant vascular sites [34]. We also identified several up-regulated genes which have not been reported to be associated with stress response, including Caudin, and Tlx2, and have been known to be harmful to cells at high expression levels. Furthermore, Aqp4 and Defb10 could be recommended as novel key elements that mediated the stress response. These might be used as new targets for the development of therapeutics for treating chronic stress or depression although further studies of the genetic and structural aspects of each target are required.

ACKNOWLEDGEMENTS

This study was financially supported by the Medicinal Crops Division, Ginseng and Medicinal Plants Research Institute Rural Development Administration (20070201030031).

REFERENCES

1. Padgett DA, Glaser R. How stress influences the immune response. Trends Immunol 2003;24:444-448.
2. Cannon WB. Organization for physiological homeostasis. Physiol Rev 1929;9:399-431.
3. Pacak K, Palkovits M. Stressor specificity of central neuroendocrine responses: implications for stress-related disorders. Endocr Rev 2001;22:502-548.
4. Yun SJ, Hahm DH, Lee EH. Immobilization stress induces the expression of alphaB-crystallin in rat hippocampus: implications of glial activation in stress-mediated hippocampal degeneration. Neurosci Lett 2002;324:45-48.
5. Rage F, Givalois L, Marmigere F, Tapia-Arancibia L, Arancibia S. Immobilization stress rapidly modulates BDNF mRNA expression in the hypothalamus of adult male rats. Neuroscience 2002;112:309-318.
6. Choi EH, Lee HJ, Kim CJ, Kim JT, Kwun IS, Kim Y. Anti-stress effects of ginseng in immobilization-stressed rats. J Food Sci Nutr 2004;9:253-258.
7. Dang H, Chen Y, Liu X, Wang Q, Wang L, Jia W, Wang Y. Antidepressant effects of ginseng total saponins in the forced swimming test and chronic mild stress models of depression. Prog Neuropsychopharmacol Biol Psychiatry 2009;33:1417-1424.
8. Cho JG, Lee MK, Lee JW, Park HJ, Lee DY, Lee YH, Yang DC, Baek NI. Physicochemical characterization and NMR assignments of ginsenosides Rb1, Rb2, Rc, and Rd isolated from Panax ginseng. J Ginseng Res 2010;34:113-121.
9. Lee SH, Jung BH, Kim SY, Lee EH, Chung BC. The antistress effect of ginseng total saponin and ginsenoside Rg3 and Rb1 evaluated by brain polyamine level under immobilization stress. Pharmacol Res 2006;54:46-49.
10. Renaud S, Hays AP, Brannagan TH 3rd, Sander HW, Edgar M, Weimer LH, Olarte MR, Dalakas MC, Xiang Z, Danon MJ, et al. Gene expression profiling in chronic inflammatory demyelinating polyneuropathy. J Neuroimmunol 2005;159:203-214.
11. Williams NM, O'Donovan MC, Owen MJ. Genome scans and microarrays: converging on genes for schizophrenia? Genome Biol 2002;3:REVIEWS1011.
12. Lee HC, Chang DE, Yeom M, Kim GH, Choi KD, Shim I, Lee HJ, Hahm DH. Gene expression profiling in hypothalamus of immobilization-stressed mouse using cDNA microarray. Brain Res Mol Brain Res 2005;135:293-300.
13. Dudoit S, Yang YH, Callow MJ, Speed TP. Statistical methods for identifying differentially expressed genes in replicated cDNA microarray experiments. Stat Sin 2002;12:111-140.
14. Kaiser V, Diamond G. Expression of mammalian defensin genes. J Leukoc Biol 2000;68:779-784.

15. Niyonsaba F, Nagaoka I, Ogawa H. Human defensins and cathelicidins in the skin: beyond direct antimicrobial properties. Crit Rev Immunol 2006;26:545-576.
16. Ren J, Davidoff AJ. alpha2-Heremans Schmid glycoprotein, a putative inhibitor of tyrosine kinase, prevents glucose toxicity associated with cardiomyocyte dysfunction. Diabetes Metab Res Rev 2002;18:305-310.
17. Nguyen-Jackson H, Panopoulos AD, Zhang H, Li HS, Watowich SS. STAT3 controls the neutrophil migratory response to CXCR2 ligands by direct activation of G-CSF-induced CXCR2 expression and via modulation of CXCR2 signal transduction. Blood 2010;115:3354-3363.
18. Gregory AD, Capoccia BJ, Woloszynek JR, Link DC. Systemic levels of G-CSF and interleukin-6 determine the angiogenic potential of bone marrow resident monocytes. J Leukoc Biol 2010;88:123-131.
19. Fujikado N, Saijo S, Yonezawa T, Shimamori K, Ishii A, Sugai S, Kotaki H, Sudo K, Nose M, Iwakura Y. Dcir deficiency causes development of autoimmune diseases in mice due to excess expansion of dendritic cells. Nat Med 2008;14:176-180.
20. Hinson ER, Joshi NS, Chen JH, Rahner C, Jung YW, Wang X, Kaech SM, Cresswell P. Viperin is highly induced in neutrophils and macrophages during acute and chronic lymphocytic choriomeningitis virus infection. J Immunol 2010; 184:5723-5731.
21. Miyajima N, Maruyama S, Nonomura K, Hatakeyama S. TRIM36 interacts with the kinetochore protein CENP-H and delays cell cycle progression. Biochem Biophys Res Commun 2009;381:383-387.
22. Nishihashi A, Haraguchi T, Hiraoka Y, Ikemura T, Regnier V, Dodson H, Earnshaw WC, Fukagawa T. CENP-I is essential for centromere function in vertebrate cells. Dev Cell 2002;2:463-476.
23. Vanden Bosch A, Raemaekers T, Denayer S, Torrekens S, Smets N, Moermans K, Dewerchin M, Carmeliet P, Carmeliet G. NuSAP is essential for chromatin-induced spindle formation during early embryogenesis. J Cell Sci 2010;123(Pt 19):3244-3255.
24. Bombardelli L, Carpenter ES, Wu AP, Alston N, DelGiorno KE, Crawford HC. Pancreas-specific ablation of beta1 integrin induces tissue degeneration by disrupting acinar cell polarity. Gastroenterology 2010;138:2531-2540, 2540.e1-4.
25. Ohlsson L, Hjelte L, Huhn M, Scholte BJ, Wilke M, Flodstrom-Tullberg M, Nilsson A. Expression of intestinal and lung alkaline sphingomyelinase and neutral ceramidase in cystic fibrosis f508del transgenic mice. J Pediatr Gastroenterol Nutr 2008;47:547-554.
26. Kono M, Dreier JL, Ellis JM, Allende ML, Kalkofen DN, Sanders KM, Bielawski J, Bielawska A, Hannun YA, Proia RL. Neutral ceramidase encoded by the Asah2 gene is essential for the intestinal degradation of sphingolipids. J Biol Chem 2006;281:7324-7331.
27. Soundararajan P, Fawcett JP, Rafuse VF. Guidance of postural motoneurons requires MAPK/ERK signaling downstream of fibroblast growth factor receptor 1. J Neurosci 2010;30:6595-6606.
28. Lu X, Su N, Yang J, Huang W, Li C, Zhao L, He Q, Du X, Shen Y, Chen B, et al. Fibroblast growth factor receptor 1 regulates the differentiation and activation of osteoclasts through Erk1/2 pathway. Biochem Biophys Res Commun 2009;390:494-499.
29. Wang SJ, Furusho M, D'Sa C, Kuwada S, Conti L, Morest DK, Bansal R. Inactivation of fibroblast growth factor receptor signaling in myelinating glial cells results in significant loss of adult spiral ganglion neurons accompanied by age-related hearing impairment. J Neurosci Res 2009; 87:3428-3437.
30. Chang R, Wang E. Mouse translation elongation factor eEF1A-2 interacts with Prdx-I to protect cells against apoptotic death induced by oxidative stress. J Cell Biochem 2007;100:267-278.
31. Ruest LB, Marcotte R, Wang E. Peptide elongation factor eEF1A-2/S1 expression in cultured differentiated myotubes and its protective effect against caspase-3-mediated apoptosis. J Biol Chem 2002;277:5418-5425.
32. Roberts SJ, Stewart AJ, Sadler PJ, Farquharson C. Human PHOSPHO1 exhibits high specific phosphoethanolamine and phosphocholine phosphatase activities. Biochem J 2004;382(Pt 1):59-65.
33. Roberts SJ, Stewart AJ, Schmid R, Blindauer CA, Bond SR, Sadler PJ, Farquharson C. Probing the substrate specificities of human PHOSPHO1 and PHOSPHO2. Biochim Biophys Acta 2005;1752:73-82.
34. Yoshida H, Russell J, Granger DN. Thrombin mediates the extraintestinal thrombosis associated with experimental colitis. Am J Physiol Gastrointest Liver Physiol 2008; 295:G904-G908.